

---

GEOMETRICAL  
AND APPLIED OPTICS

---

## Immersion Clearing of Human Blood in the Visible and Near-Infrared Spectral Regions

A. N. Bashkatov, D. M. Zhestkov, É. A. Genina, and V. V. Tuchin

*Chernyshevsky State University, Saratov, 410012 Russia*

Received June 21, 2004

**Abstract**—The possibility of the immersion clearing of human blood in the visible and near-IR spectral regions is considered and theoretically substantiated. On the basis of the model presented, the spectral behavior of the scattering and absorption characteristics of blood upon its immersion clearing by glucose is analyzed. © 2005 Pleiades Publishing, Inc.

### INTRODUCTION

One of the avenues of research in biomedical optics is the advancement of techniques for probing of biological tissues with visible and near-IR radiation, which allows imaging of their structure [1–3]. This interest stems from the possibility of developing a harmless and versatile tool for the diagnostics of biological tissues. At present, the majority of the existing methods use the so-called transparency window for the optical probing of biological tissues, which occupies the wavelength range from 650 to 1200 nm [2]. The use of visible light for diagnostics of biological tissues is complicated by its absorption by various chromophores of tissues, the most important of which in this spectral range is blood, having clearly pronounced absorption and scattering properties [4–8]. Therefore, the possibility of controlling in vivo the optical parameters of blood will enable a considerable increase in the sensitivity of such methods of optical diagnostics as fluorescent and confocal spectroscopy [9–11], optical coherence tomography [12–14], spatially resolved reflectance spectroscopy [15–18], and so on. An efficient method of considerably decreasing light scattering is optical immersion, i.e., matching of the refractive indices of the scattering centers and the base substance by means of introduction of corresponding preparations into a biological tissue. Studies have shown that the use of aqueous solutions of glucose, propylene glycol, trazograph, glycerin, etc., as immersion liquids makes it possible to considerably decrease (by several times) the scattering power of biological tissues [1, 3, 9–30]. Similar results have been obtained for whole blood [14, 31–36]. At the same time, at present, the influence of immersion liquids on the optical, in particular, scattering, characteristics of blood remains insufficiently studied.

The objective of this study is to analyze the possibility of considerably decreasing the scattering power of blood upon its immersion clearing by glucose in the spectral range 400–1000 nm.

### AN OPTICAL MODEL OF BLOOD

Optically, whole blood is a highly concentrated turbid medium consisting of plasma (55 vol %) and blood corpuscles (45 vol %) [4–6], 99% of which are erythrocytes and the remaining 1% of which are leukocytes and thrombocytes [5, 6]. Because of this, the optics of whole blood is determined mainly by the optical properties of erythrocytes and plasma, whereas the contribution to scattering from the remaining blood corpuscles can be neglected. The analysis of the propagation and scattering of radiation in such a medium is reduced to considering the scattering and absorption characteristics of an individual particle and taking into account the concentration effects and polydispersity of the suspension.

The relationships that determine the propagation of light in biological tissues and fluids (in this case, in blood) can be described on the basis of the notion of radiation transfer in randomly inhomogeneous media. At present, the most widespread approach to the description of this phenomenon is the theory of radiation transfer [1]. To describe the radiation transfer process in biological tissues, this theory uses such quantities as the absorption coefficient  $\mu_a$ , the scattering coefficient  $\mu_s$ , and the anisotropy factor  $g$  (the average cosine of the scattering angle) of an elementary volume of the medium under study. In turn, these characteristics are determined by the size of erythrocytes, as well as the real ( $n$ ) and the imaginary ( $\chi$ ) parts of the complex refractive index ( $n + i\chi$ ) of the scattering particles (erythrocytes) and their environment (blood plasma).

Under normal physiological conditions, human erythrocytes are anucleate cells in the form of biconcave disks with a diameter ranging between 5.7 and 9.3  $\mu\text{m}$  (the average value is about 7.5  $\mu\text{m}$ ) [6] and a maximal thickness varying between 1.7 and 2.4  $\mu\text{m}$  [37]. The average volume of an erythrocyte amounts to about 90  $\mu\text{m}^3$  [4, 5, 7, 8] and, according to different data, varies between 70 and 100 [37], 50 and 200 [7], or

30 and 150  $\mu\text{m}^3$  [8]. In the presence of different pathologies, as well as upon changes in the osmolarity or pH of the blood plasma, normal erythrocytes (discocytes) can change in shape without changing in volume [6, 37]. An erythrocyte consists of a membrane (with a thickness of from 7 [8] to 25 nm [37]) and cytoplasm, which is mainly an aqueous solution of hemoglobin [8, 38]. The concentration of hemoglobin in completely hemolyzed blood varies from 134 to 173 g/l [4], while the concentration of hemoglobin in erythrocytes varies from 300 to 360 g/l, with the average concentration being equal to 340 g/l [8]. The content of salts in the erythrocyte cytoplasm is about 7 g/l; the concentration of other organic components (lipids, sugars, enzymes, and proteins) is approximately equal to 2 g/l [8].

The phase function and scattering cross section of an individual erythrocyte depend on its orientation [6]. However, the light scattering from a large number of randomly distributed nonspherical particles is the same as the scattering from a system of randomly distributed spherical particles of equivalent volume [39, 40]. Therefore, in our model, erythrocytes are represented as absorbing and scattering homogeneous spherical particles, with the volume of each such particle being equal to the volume of a real erythrocyte. In calculations, the contribution to the scattering from the erythrocyte membranes was neglected due to their small thickness [8].

The polydispersity of the erythrocytes was taken into account based on the data obtained in [7] (Fig. 1). The total volume concentration of erythrocytes in the blood (the hematocrit value) is equal to 45%, which corresponds to the hematocrit of the venous blood of a man [4, 41]. The fact that the distribution function exhibits the presence of particles whose volume considerably exceeds the volume of a normal erythrocyte is associated with the aggregation of erythrocytes into large-size clusters, which, along with individual erythrocytes, contribute to the scattering spectrum of whole blood [42].

It was shown that the concentration of hemoglobin in erythrocytes directly correlates with their volume [8]. According to the data obtained in that study, the concentration of hemoglobin can be related to the erythrocyte volume as

$$C_{\text{Hb}} = 0.72313 - 0.00451V, \quad (1)$$

where  $C_{\text{Hb}}$  is the concentration of hemoglobin (g/ml) and  $V$  is the erythrocyte volume ( $\mu\text{m}^3$ ).

The spectral dependences of the real ( $n$ ) and imaginary ( $\chi$ ) parts of the complex refractive index of the erythrocytes are shown in Fig. 2 [6]. The degree of oxygenation is equal to 100%, and the concentration of hemoglobin amounts to 2.036 mM [6].

Both the real and the imaginary parts of the refractive index of erythrocytes are directly proportional to

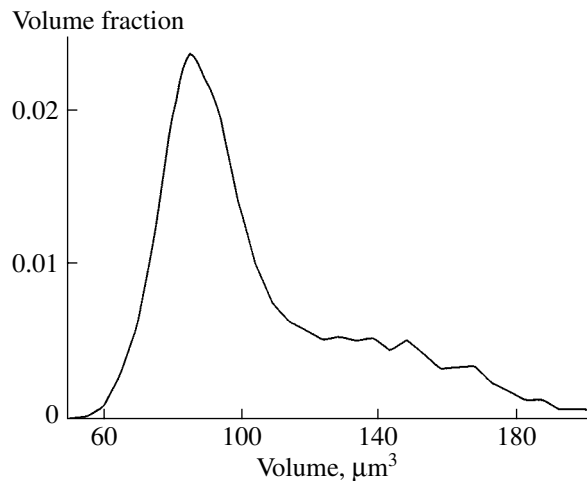


**Fig. 1.** Size distribution of spherical particles modeling the erythrocytes [7]. The total volume fraction of the erythrocytes in the blood (hematocrit) is 45%.

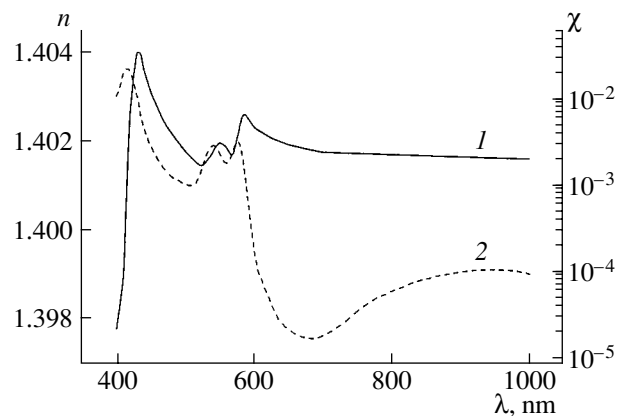


**Fig. 2.** Spectral dependences of the (1) real  $n$  and (2) imaginary  $\chi$  parts of the complex refractive index of erythrocytes [6].

the hemoglobin concentration in erythrocytes [4, 6]; i.e.,

$$n_e = n_0 + \alpha C_{\text{Hb}}, \quad (2)$$

$$\chi_e = \beta C_{\text{Hb}}, \quad (3)$$

where  $n_0 = 1.34$  is the refractive index of the erythrocyte cytoplasm [8] and  $\alpha$  and  $\beta$  are spectrally dependent coefficients. For the wavelength of 589 nm,  $\alpha = 0.1942$  ml/g [4], while, for the wavelength 640 nm,  $\alpha = 0.284$  ml/g and  $\beta = 0.0001477$  ml/g [6]. Since the content of salts, sugars, and other organic components in the erythrocyte cytoplasm is insignificant, we assumed in our calculations that the spectral dependence of the erythrocyte cytoplasm correlates with the spectral dependence of the refractive index of water, i.e.,

$n_0(\lambda) = n_w(\lambda) + 0.007$ . The spectral dependence of the refractive index of water is determined by the expression  $n_w(\lambda) = 1.31848 + 6.662/(\lambda - 129.2)$  ( $\lambda$  is expressed in nanometers) [43]. The spectral dependences of the coefficients  $\alpha$  and  $\beta$  were calculated on the basis of the data of Fig. 2 in [6] and using a value of the hemoglobin concentration in erythrocytes equal to 322 g/l, which was obtained from Eq. (2) with the coefficient  $\alpha = 0.1942$  ml/g.

The blood plasma contains up to 91% water, 6.5–8% (about 70 g/l) proteins (hemoglobin, albumin, and globulin), and about 2% low-molecular-weight compounds [34].

The spectral dependence of the real part of the refractive index of the blood plasma ( $n_p$ ) in the spectral range 488–1341 nm is determined by the expression  $n_p = 1.3194 + 1.4578 \times 10^{-2}/\lambda^2 - 1.7383 \times 10^{-3}/\lambda^4$ , where  $\lambda$  is the wavelength ( $\mu\text{m}$ ) [44]. To perform the calculations, this dependence was extrapolated to the range from 400 to 1000 nm,

$$n_p = 1.3254 + 8.4052 \times 10^3/\lambda^2 - 3.9572 \times 10^8/\lambda^4 - 2.3617 \times 10^{13}/\lambda^6, \quad (4)$$

where  $\lambda$  is the wavelength (nm). Since the blood plasma does not have pronounced absorption bands in this spectral range, we neglected the imaginary part of the refractive index of the plasma in our calculations.

In terms of the Mie theory, the scattering and absorption cross sections ( $\sigma_s$  and  $\sigma_a$ , respectively) and the anisotropy factor of a homogeneous sphere are expressed as [45]

$$\sigma_s = \frac{\lambda^2}{2\pi n_p^2} \sum_{n=1}^{\infty} (2n+1)(|a_n|^2 + |b_n|^2), \quad (5)$$

$$\sigma_a = \frac{\lambda^2}{2\pi n_p^2} \sum_{n=1}^{\infty} (2n+1) \times [\text{Re}(a_n + b_n) - (|a_n|^2 + |b_n|^2)], \quad (6)$$

$$g = \frac{\lambda^2}{\pi n_p^2 \sigma_s} \left[ \sum_{n=1}^{\infty} \frac{n(n+2)}{n+1} \text{Re}\{a_n a_{n+1}^* + b_n b_{n+1}^*\} + \sum_{n=1}^{\infty} \frac{2n+1}{n(n+1)} \text{Re}\{a_n b_n^*\} \right], \quad (7)$$

where  $a_n$  and  $b_n$  are the Mie coefficients and  $a_n^*$ , and  $b_n^*$  are their complex conjugates. The expressions for  $a_n$  and  $b_n$  are given by

$$a_n = \frac{m\Psi_n(mx)\Psi_n'(x) - \Psi_n(x)\Psi_n'(mx)}{m\Psi_n(mx)\xi_n'(x) - \xi_n(x)\Psi_n'(mx)},$$

$$b_n = \frac{\Psi_n(mx)\Psi_n'(x) - m\Psi_n(x)\Psi_n'(mx)}{\Psi_n(mx)\xi_n'(x) - m\xi_n(x)\Psi_n'(mx)}.$$

Here,  $m = (n_e + i\chi_e)/n_p$  and  $x = 2\pi n_p a/\lambda$  are the relative refractive index and the diffraction size of the erythrocyte, respectively,  $a$  is the erythrocyte radius, and  $\Psi_n(\rho) = \rho J_n(\rho)$  and  $\xi_n(\rho) = \rho H_n^{(1)}(\rho)$  are the Riccati–Bessel functions, where  $J_n(\rho)$  is the Bessel function of the first kind of the  $n$ th order and  $H_n^{(1)}(\rho)$  is the Bessel function of the third kind of the  $n$ th order.

According to [46], the scattering and absorption coefficients and the anisotropy factor of whole blood considered as a system of closely packed polydisperse particles are given by

$$\mu_s = (1-H) \sum_{i=1}^M N_i \sigma_{s_i}, \quad (8)$$

$$\mu_a = \sum_{i=1}^M N_i \sigma_{a_i}, \quad (9)$$

$$g = \sum_{i=1}^M \mu_{s_i} g_i / \sum_{i=1}^M \mu_{s_i}. \quad (10)$$

Here,  $H$  is the hematocrit value;  $M$  is the number of volume fractions of erythrocytes (in this study,  $M = 150$ );  $N_i = C_i/V_{ei}$  is the number of particles per unit volume of the medium;  $C_i$  is the volume fraction occupied by particles of the  $i$ th diameter (Fig. 1); and  $V_{ei} = 4\pi a_i^3/3$  is the erythrocyte volume. In Eq. (8), the necessity of introduction of the factor  $(1-H)$  [5, 7, 47], which is called the packing factor of scatterers, is determined by interference effects of radiation scattered from neighboring particles.

#### MODELING OF THE OPTICAL CLEARING OF BLOOD UPON INTRODUCTION OF GLUCOSE INTO THE BLOOD PLASMA

The use of aqueous solutions of glucose as immersion agents for the optical clearing of biological tissues showed their high efficiency [9, 15–17, 19, 23, 25–27]. In view of the data obtained in [31, 32, 34, 36], one should expect a considerable decrease in the scattering power of blood in the visible and near-IR spectral ranges upon partial replacement of the blood plasma by glucose solutions of different concentrations. Upon introduction of glucose into blood, the refractive index of the blood plasma increases and becomes comparable with that of erythrocytes. As a consequence, the scattering coefficient decreases, while the blood anisotropy factor increases. Within the framework of this study, we do not consider particular techniques for the clinical

application of the optical immersion of blood corpuscles. At the same time, we suggest that intravenous injection of glucose aqueous solutions could be the most suitable method since this technique is already used in clinical practice [48].

The spectral dependence of the refractive index of an aqueous glucose solution is defined by the expression  $n_{gl} = n_w + 0.1515C_{gl}$  [31], where  $C_{gl}$  is the glucose concentration (g/ml). By analogy with this expression, we will define the refractive index of a glucose solution in the blood plasma as

$$n_p^{im}(\lambda) = n_p(\lambda) + 0.1515C_{gl}, \quad (11)$$

where  $n_p(\lambda)$  is the refractive index of the blood plasma determined by Eq. (4).

Since glucose does not have absorption bands in the spectral range under consideration, we assume that, after being introduced into blood, glucose has no effect on the blood absorption. In addition, as a first approximation, it is assumed that glucose molecules do not bind with proteins of the blood plasma.

A change in the osmolarity of the plasma leads to changes in the size and the complex refractive index of the blood corpuscles due to their osmotic dehydration [4, 49] and, consequently, to changes in their scattering and absorption powers. Normally, the osmolarity of blood amounts to 280–300 mosm/l [4, 50]. The introduction of glucose into the blood plasma leads to a linear increase in the osmolarity, which reaches the value 6000 mosm/l at a glucose concentration in the blood plasma of about 1 g/ml.

On the basis of the data of [4], the change in the volume of erythrocytes was described by the following empirical expression:

$$V(\text{osm}) = V_0(0.463 + 1.19 \exp(-\text{osm}/376.2)), \quad (12)$$

where osm is the blood osmolarity (mosm/l),  $V$  is the erythrocyte volume ( $\mu\text{m}^3$ ) for the given value of the blood osmolarity, and  $V_0$  is the erythrocyte volume at a blood osmolarity equal to 300 mosm/l. Upon introduction of glucose into the blood plasma, the hematocrit of the blood decreases. The value of this parameter is successively equal to 45% at osm = 300 mosm/l ( $C_{gl} = 0$  g/l), 32% at osm = 580 mosm/l ( $C_{gl} = 0.05$  g/ml), 26% at osm = 850 mosm/l ( $C_{gl} = 0.1$  g/ml), and 22% at osm = 1400 mosm/l ( $C_{gl} = 0.2$  g/ml). On a further increase in the glucose concentration in the plasma ( $C_{gl} = 0.3$ –1 g/ml), the hematocrit becomes equal to about 21% and, despite an increase in the blood osmolarity (osm = 2000–6000 mosm/l), this value of the hematocrit does not change. In modeling, we assumed that the shape of the size distribution function of erythrocytes does not change.

The osmotic dehydration leads to an increase in the concentration of hemoglobin in blood and, as a consequence, to an increase in both the real and the imagi-

nary parts of the refractive index of erythrocytes. The change in the erythrocyte volume was calculated by Eq. (12). The changes in the real and imaginary parts of the refractive index were estimated by Eqs. (2) and (3) taking into account the change in the hemoglobin concentration determined by Eq. (1).

The coefficients of scattering and absorption and the anisotropy factor of whole blood both under normal conditions (the hematocrit is equal to 45%) and upon immersion clearing by glucose were calculated from expressions (8)–(10). In these calculations, the cross sections of scattering and absorption and the anisotropy factor of an individual erythrocyte were determined using expressions (5)–(7). The spectral dependences of the real and imaginary parts of the refractive index of erythrocytes under normal conditions were calculated according to formulas (2) and (3) taking into account the size distribution function of erythrocytes (Fig. 1 in [7]) and Eq. (1). The spectral dependence of the refractive index of the blood plasma in relation to the glucose concentration was calculated by formula (11), in which the spectral dependence of the refractive index of the blood plasma prior to the introduction of glucose was found from extrapolation formula (4).

It should be noted that these estimates may somewhat differ from those observed in vivo since, in our calculations, we disregarded the effect of the blood flow, which, according to [4], leads to a decrease in both the scattering and the absorption power of blood. In addition, it seems that the changes in the erythrocyte volume and the blood hematocrit will differ from those used in our modeling since the blood flow will reduce the glucose concentration, as a result of which the changes in the erythrocyte volume and the blood hematocrit will be much less pronounced.

## RESULTS AND DISCUSSION

To test our model, we calculated the absorption and scattering spectra of blood in the range from 400 to 1000 nm for a hematocrit value equal to 5% and compared these calculations with the experimental data obtained in [4]. It is seen from this figure that the calculated and experimentally measured absorption spectra are practically identical to each other. The agreement between the theoretical and observed scattering spectra is somewhat worse. According to the data of [4], the scattering spectrum of blood exhibits a peak in the range 440–600 nm, located at 500 nm, which we failed to reproduce in terms of our model. This can be explained by the simplicity of our model, in particular, by the fact that the polydispersity of the system is likely to be considered inadequately. The second reason could be possible errors in the quantization of the experimental data. Apart from this, a lack of information about the distribution function of erythrocytes and about the hemoglobin concentration in the experimental samples is also a reason why we were unable to reproduce completely the experimental scattering spectrum. At the

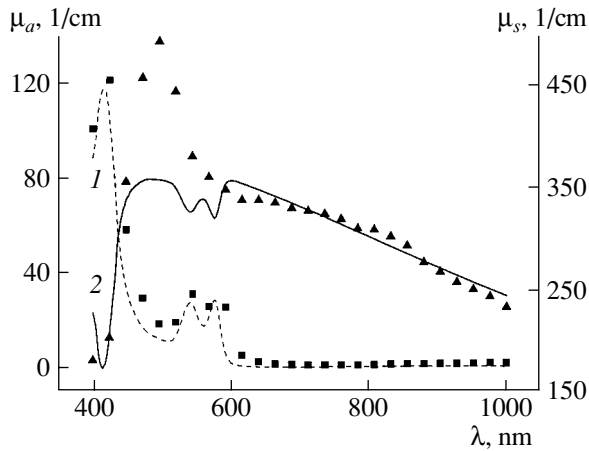


**Fig. 3.** Spectra of (1) absorption and (2) scattering of blood calculated in the context of the proposed model for a hematocrit value of 5%. The squares and triangles show, respectively, the absorption and scattering spectra experimentally measured in [4].

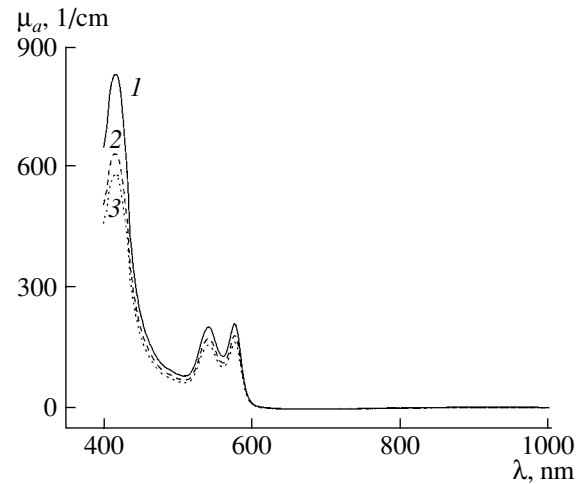


**Fig. 4.** Absorption spectra of blood upon its immersion clearing by glucose calculated in the context of the model presented. The glucose concentration is  $C_{gl} = (1) 0, (2) 0.5,$  and (3) 1 g/ml.

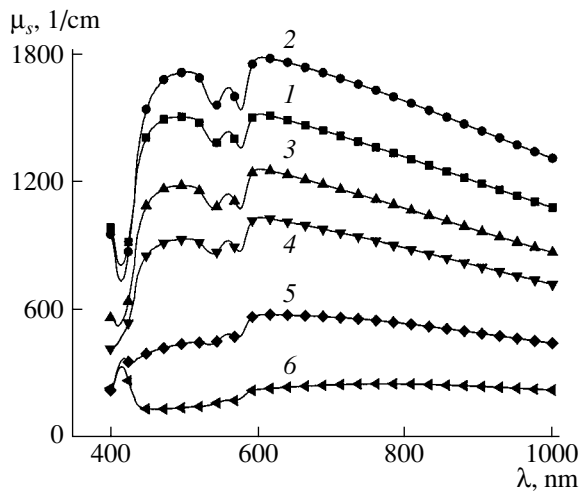


**Fig. 5.** Calculated scattering spectra of blood upon its immersion clearing by glucose in the case where the refractive index of the blood plasma is less than that of the erythrocytes. The glucose concentration in the blood plasma is  $C_{gl} = (1) 0, (2) 0.1, (3) 0.25, (4) 0.3, (5) 0.4,$  and (6) 0.5 g/ml.

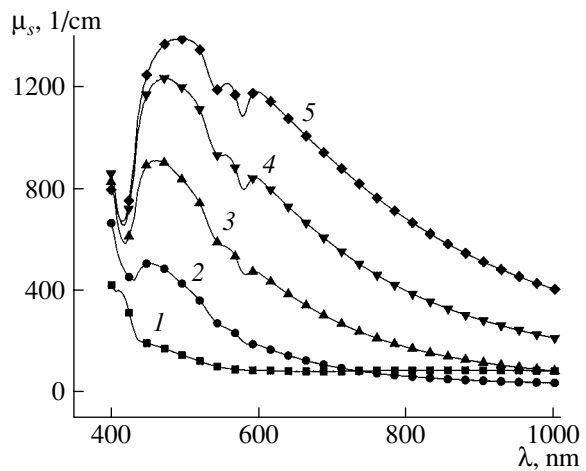


**Fig. 6.** Calculated scattering spectra of blood upon its immersion clearing by glucose in the case where the refractive index of the blood plasma is greater than that of the erythrocytes. The glucose concentration in the blood plasma is  $C_{gl} = (1) 0.6, (2) 0.7, (3) 0.8, (4) 0.9,$  and (5) 1.0 g/ml.

same time, in the ranges 400–440 and 600–1000 nm, the calculated and experimental scattering spectra almost completely coincide with each other. Therefore, the comparison between the calculated and experimental data shows that the optical model of blood presented can fairly reliably describe the optical characteristics of blood in the spectral range under consideration, including the changes in these characteristics upon immersion clearing of blood.

Figure 4 shows the spectral dependence of the absorption coefficient of whole blood upon its immer-

sion clearing by glucose. It is seen that the changes in the absorption spectrum of blood are insignificant and localized mainly in the absorption bands of hemoglobin at 415 (the Soret band), 542, and 575 nm (the  $\alpha$  and  $\beta$  bands, respectively). It is also seen that the influence of the immersion agent manifests itself in a uniform decrease in the absorption coefficient with increasing glucose concentration in the blood plasma.

The influence of glucose as an immersion agent on the scattering characteristics of blood is much more considerable (Figs. 5–10). Figures 5 and 6 show the

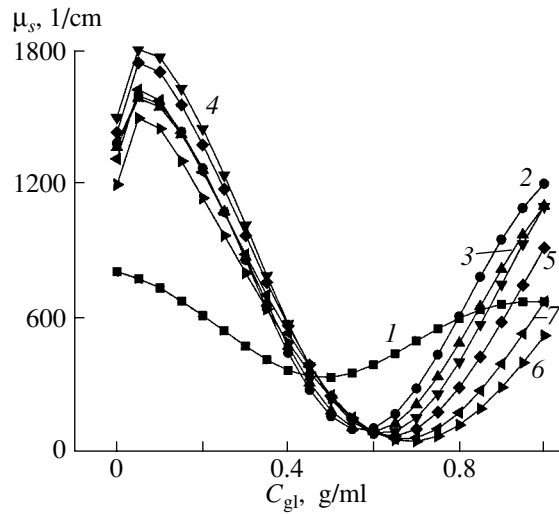


**Fig. 7.** Dependence of the scattering coefficient of blood on the glucose concentration.  $\lambda = (1)$  415, (2) 542, (3) 575, (4) 633, (5) 700, (6) 805, and (7) 900 nm.

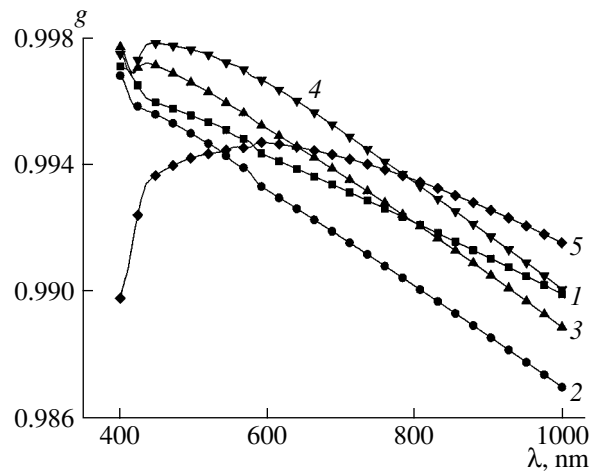


**Fig. 8.** Calculated spectral dependence of the scattering anisotropy factor of blood upon its immersion clearing by glucose.  $C_{gl} = (1)$  0, (2) 0.2, (3) 0.4, (4) 0.6, and (5) 1.0 g/ml.

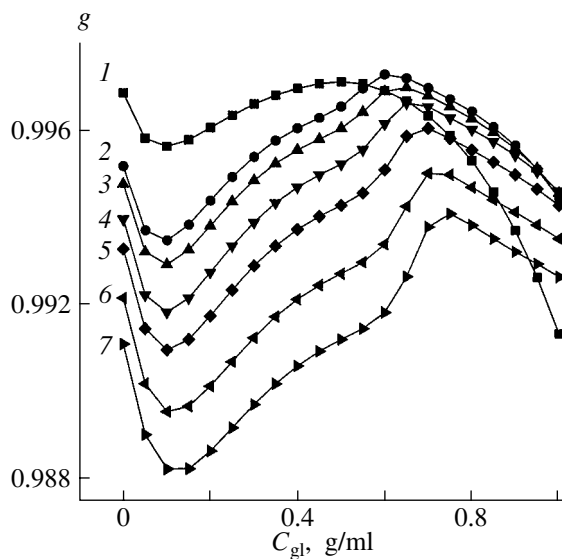


**Fig. 9.** Dependence of the scattering anisotropy factor of blood on the glucose concentration.  $\lambda = (1)$  415, (2) 542, (3) 575, (4) 633, (5) 700, (6) 805, and (7) 900 nm.

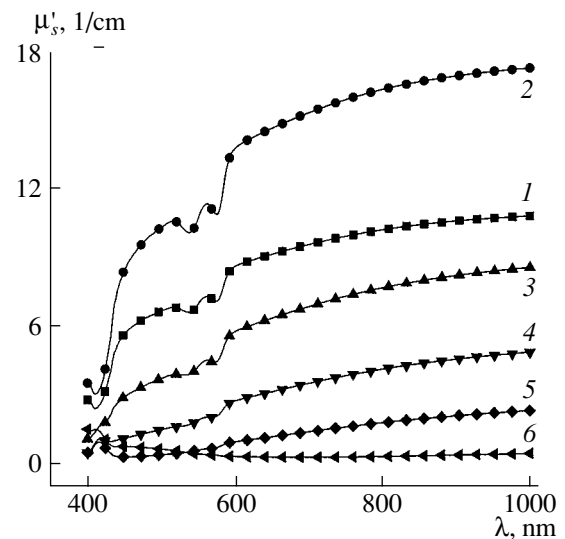


**Fig. 10.** Calculated spectra of the transport scattering coefficient of blood upon its immersion clearing by glucose.  $C_{gl} = (1)$  0, (2) 0.1, (3) 0.3, (4) 0.4, (5) 0.5, and (6) 0.65 g/ml.

scattering spectra of blood at different content of glucose in the blood plasma. The shape of the scattering spectra is determined by the influence of the absorption bands of hemoglobin, which manifests itself as valleys in the scattering spectrum in the ranges of these absorption bands. It is seen from the spectra presented that the valleys located at 415, 542, and 575 nm shallow with increasing glucose concentration. The spectral dependence of the scattering coefficient becomes more monotonic. On the whole, as the glucose concentration

in the blood plasma increases, the scattering coefficient considerably decreases in the entire spectral interval (by approximately 15 times). In the spectral range of the Soret band, the scattering coefficient attains its minimum value at a glucose concentration of 0.5 g/ml (Fig. 7), while, in the remaining part of the spectrum, this minimum is reached at a glucose concentration within 0.6–0.65 g/ml. On further increase in the glucose concentration the scattering coefficient increases in the entire spectral range. The increase in the scatter-

ing coefficient observed at small glucose concentrations (Fig. 7) is related to an increase in the refractive index of the erythrocytes, which is caused by an increase in the hemoglobin concentration due to the osmotic dehydration of erythrocytes. The dependence of the scattering coefficient on the glucose concentration presented in Fig. 7 shows that the optical clearing of blood occurs nonuniformly in different spectral ranges. Thus, the maximal reduction in the scattering in the range of the Soret band (415 nm) is observed at a glucose concentration of 0.5 g/ml, whereas, on passage to a longer wavelength range of the spectrum, the immersion clearing of blood occurs at higher glucose concentrations. In particular, for the wavelength 900 nm, the maximal decrease in the scattering occurs at a glucose concentration equal to 0.7 g/ml. For the wavelengths 542 and 575 nm, the maximal clearing is observed at glucose concentrations of 0.55 and 0.6 g/ml, respectively. For the wavelength 633 nm, which is the most frequently used in laser irradiation of blood [3], the minimum in the light scattering is also observed at a glucose concentration of 0.6 g/ml, whereas, for the wavelength 805 nm (the isobestic point of hemoglobin [3]), the minimal light scattering occurs at the concentration 0.65 g/ml. The wavelengths 700 and 900 nm were chosen because the effect of the imaginary part of the refractive index of hemoglobin at these wavelengths is minimal. The optimal concentration of glucose for the wavelength 700 nm is equal to 0.65 g/ml.

According to the Mie theory [45], the main parameter that determines the value of the scattering coefficient is the relative refractive index, defined as the ratio of the complex refractive index of the erythrocytes to the refractive index of the blood plasma. In accordance with this, an increase in the refractive index of the plasma leads to a decrease in both the real and the imaginary parts of the relative refractive index of the erythrocytes. This circumstance causes the coefficients of absorption and scattering of blood to decrease (Figs. 4, 5). Apart from this, the decrease in the scattering and absorption coefficients is related with a decrease in the hematocrit of blood caused by the osmotic dehydration of erythrocytes. However, beginning from a glucose concentration of 0.3 g/ml, the hematocrit virtually does not change and the decrease in the scattering and absorption is connected only with the immersion effect. When the glucose concentration exceeds 0.7 g/ml, the refractive index of the plasma becomes greater than that of the erythrocytes and, as a consequence, the scattering coefficient increases.

It is interesting to note the influence of immersion on the behavior of the scattering characteristics of blood in the range of the strong absorption bands. As the glucose concentration, i.e., the refractive index of the blood plasma, increases, the depth of the valley in the scattering spectrum in the range of the Soret band decreases and then, when the refractive index of the plasma becomes comparable with the real part of the complex refractive index of the erythrocytes, a peak

arises in this spectral range, whose shape and magnitude are determined by the imaginary part of the complex refractive index of the erythrocytes.

Figures 8 and 9 show the blood anisotropy factor in relation to the wavelength and the glucose concentration in the blood plasma. It is seen that, as the wavelength increases, the anisotropy factor insignificantly decreases (from 0.997 at 400 nm to 0.99 at 1000 nm). At small glucose concentrations in the blood plasma (up to 0.1 g/ml), the anisotropy factor decreases in the entire spectral range under consideration, which is caused by the osmotic compression of erythrocytes (Fig. 9). As the glucose concentration in the blood plasma increases (from 0.1 to 0.6–0.7 g/ml), the anisotropy factor increases in the entire spectral range, which is caused by the immersion effect. This manifestation of the immersion action of glucose is very important for optical tomography and therapy since an increase in the anisotropy factor implies an increase in the depth of penetration of light into a biological tissue upon its optical probing. As in the previous case, a glucose concentration within 0.6–0.7 g/ml is optimal. On a further increase in the glucose concentration in the blood plasma, the anisotropy factor decreases. It is also necessary note the appearance of a valley in the spectrum of the anisotropy factor in the range of the Soret absorption band at 415 nm. The occurrence of this valley is associated with the influence of the imaginary part of the complex refractive index on the formation of the scattering spectrum under conditions of immersion clearing of erythrocytes.

The transport scattering coefficient  $\mu'_s = \mu_s(1 - g)$  is the quantity directly determined upon solution of many inverse problems of biomedical optics. Therefore, we studied the influence of glucose on the transport scattering coefficient of blood. Figure 10 shows that, upon introduction of glucose into the blood plasma, the behavior of the spectra of the transport scattering coefficient in the entire spectral range under consideration is, on the whole, similar to the behavior of the spectra of the scattering coefficient (Figs. 5–7). The only difference in the behavior of these spectra is that the valley in the spectra of the transport scattering coefficient is shifted to the range around 410 nm as compared to its position in the scattering spectrum (at 415 nm). This difference is explained by distinctions in the spectral dependences of the scattering coefficient and the anisotropy factor of blood. The maximal optical clearing is observed at a glucose concentration of 0.65 g/ml.

## CONCLUSIONS

The aim of our model calculations was to study the possibility of using glucose for immersion clearing of blood.

We showed that the action of glucose on human whole blood made it possible to efficiently control the absorption and the scattering characteristics of blood in

a wide wavelength range. The efficiency of such control is determined by the possibility of matching of the refractive indices of the blood corpuscles (erythrocytes) and the base substance (plasma) of blood. From the viewpoint of matching refractive indices and changing the scattering properties of substances, the results presented are general for many scattering objects of biological origin.

The optical model of blood presented agrees fairly well with known experimental data and makes it possible to simulate changes in the absorption and scattering characteristics of blood, including the changes occurring upon its immersion clearing.

On the basis of our model, we analyzed the spectral behavior of the scattering and absorption characteristics of blood upon its immersion clearing by glucose. We showed that the optimal glucose concentration in the blood plasma for the optical clearing of blood is about 0.65 g/ml.

#### ACKNOWLEDGMENTS

This study was supported by a grant from the Ministry of Education of the Russian Federation for the support of leading scientific and pedagogical collectives (project no. 01.2003.15221), by the Ministry of Industry and Science of the Russian Federation (contract no. 40.018.1.1.1314), and by the U.S. Civilian Research & Development Foundation (grant no. REC-006 and BRHE Award Annex no. 07).

#### REFERENCES

- V. V. Tuchin, *Usp. Fiz. Nauk* **167**, 517 (1997) [*Phys. Usp.* **40**, 495 (1997)].
- D. A. Zimnyakov and V. V. Tuchin, *Kvantovaya Élektron. (Moscow)* **32**, 849 (2002).
- V. V. Tuchin, *Lasers and Fiber Optics in Biomedical Research* (Sarat. Gos. Univ., Saratov, 1998) [in Russian].
- A. Roggan, M. Friebel, K. Dorschel, *et al.*, *J. Biomed. Opt.* **4**, 36 (1999).
- A. N. Yaroslavsky, A. V. Priezhev, J. Rodriguez, I. V. Yaroslavsky, and H. Battarbee, in *Handbook of Optical Biomedical Diagnostics*, Ed. by V. V. Tuchin (SPIE, Bellingham, 2002), Vol. PM107, p. 169.
- A. G. Borovoi, E. I. Naats, and U. G. Opperl, *J. Biomed. Opt.* **3**, 364 (1998).
- M. Hammer, D. Schweitzer, B. Michel, *et al.*, *Appl. Opt.* **37**, 7410 (1998).
- D. H. Tycko, M. H. Metz, E. A. Epstein, and A. Grinbaum, *Appl. Opt.* **24**, 1355 (1985).
- G. Vargas, K. F. Chan, S. L. Thomsen, and A. J. Welch, *Lasers Surg. Med.* **29**, 213 (2001).
- I. V. Meglinskiĭ, A. N. Bashkatov, É. A. Genina, *et al.*, *Kvantovaya Élektron. (Moscow)* **32**, 875 (2002).
- I. V. Meglinski, A. N. Bashkatov, E. A. Genina, *et al.*, *Laser Phys.* **13**, 65 (2003).
- D. A. Zimnyakov, I. L. Maksimova, and V. V. Tuchin, *Opt. Spektrosk.* **88**, 1026 (2000) [*Opt. Spectrosc.* **88**, 936 (2000)].
- R. K. Wang, V. V. Tuchin, X. Xu, and J. B. Elder, *J. Opt. Soc. Am. B* **18**, 948 (2001).
- R. K. Wang and V. V. Tuchin, *J. X-Ray Sci. Technol.* **10**, 167 (2002).
- A. N. Bashkatov, V. V. Tuchin, E. A. Genina, *et al.*, *Proc. SPIE* **3591**, 311 (1999).
- V. V. Tuchin, A. N. Bashkatov, É. A. Genina, *et al.*, *Pis'ma Zh. Tekh. Fiz.* **27** (12), 10 (2001) [*Tech. Phys. Lett.* **27**, 489 (2001)].
- A. N. Bashkatov, E. A. Genina, and V. V. Tuchin, in *Perspectives in Engineering Optics*, Ed. by K. Singh and V. K. Rastogi (Anita, New Delhi, 2002), p. 313.
- D. Y. Churmakov, I. V. Meglinski, and D. A. Greenhalgh, *Phys. Med. Biol.* **47**, 4271 (2002).
- V. V. Tuchin, I. L. Maksimova, D. A. Zimnyakov, *et al.*, *J. Biomed. Opt.* **2**, 401 (1997).
- G. Vargas, E. K. Chan, J. K. Barton, *et al.*, *Lasers Surg. Med.* **24**, 133 (1999).
- I. L. Maksimova, D. A. Zimnyakov, and V. V. Tuchin, *Opt. Spektrosk.* **89**, 86 (2000) [*Opt. Spectrosc.* **89**, 78 (2000)].
- A. N. Bashkatov, E. A. Genina, I. V. Korovina, *et al.*, *Proc. SPIE* **4224**, 300 (2000).
- A. N. Bashkatov, E. A. Genina, I. V. Korovina, *et al.*, *Proc. SPIE* **4241**, 223 (2001).
- R. K. Wang and J. B. Elder, *Lasers Surg. Med.* **30**, 201 (2002).
- A. N. Bashkatov, É. A. Genina, Yu. P. Sinichkin, *et al.*, *Biofizika* **48**, 309 (2003).
- A. N. Bashkatov, E. A. Genina, Yu. P. Sinichkin, *et al.*, *Biophys. J.* **85**, 3310 (2003).
- E. I. Galanzha, V. V. Tuchin, A. V. Solovieva, *et al.*, *Appl. Phys. D* **36**, 1739 (2003).
- J. A. Viator, B. Choi, G. M. Peavy, *et al.*, *Phys. Med. Biol.* **48**, N15 (2003).
- X. Xu and R. K. Wang, *Phys. Med. Biol.* **49**, 457 (2004).
- M. H. Khan, B. Choi, S. Chess, *et al.*, *Lasers Surg. Med.* **34**, 83 (2004).
- J. S. Maier, S. A. Walker, S. Fantini, *et al.*, *Opt. Lett.* **19**, 2062 (1994).
- J. T. Bruulsema, J. E. Hayward, T. J. Farrell, *et al.*, *Opt. Lett.* **22**, 190 (1997).
- M. Brezinski, K. Saunders, C. Jesser, *et al.*, *Circulation* **103**, 1999 (2001).
- V. V. Tuchin, X. Xu, and R. K. Wang, *Appl. Opt.* **41**, 258 (2002).
- X. Xu, R. K. Wang, J. B. Elder, and V. V. Tuchin, *Phys. Med. Biol.* **48**, 1205 (2003).
- K. V. Larin, M. Motamedi, T. V. Ashitkov, and R. O. Esenaliev, *Phys. Med. Biol.* **48**, 1371 (2003).
- M. Yu. Kirillin and A. V. Priezhev, *Kvantovaya Élektron. (Moscow)* **32**, 883 (2002).
- V. A. Levto, S. A. Regirer, and I. Kh. Shadrina, *Rheology of Blood* (Meditsina, Moscow, 1982) [in Russian].
- N. G. Khlebtsov and S. Yu. Shchegolev, *Opt. Spektrosk.* **42**, 956 (1977) [*Opt. Spectrosc.* **42**, 549 (1977)].

40. N. G. Khlebtsov and S. Yu. Shchegolev, *Opt. Spektrosk.* **42**, 1152 (1977) [*Opt. Spectrosc.* **42**, 663 (1977)].
41. V. I. Kochubeĭ and Yu. G. Konyukhova, *Methods of Spectral Studies of Blood and Marrow of Bone* (Sarat. Gos. Univ., Saratov, 2000) [in Russian].
42. A. Ya. Khaĭrullina and S. F. Shumilina, *Zh. Prikl. Spektrosk.* **19**, 340 (1973).
43. M. Kohl, M. Cope, M. Essenpreis, and D. Bocker, *Opt. Lett.* **19**, 2170 (1994).
44. S. Cheng, H. Y. Shen, G. Zhang, *et al.*, *Proc. SPIE* **4916**, 172 (2002).
45. C. F. Bohren and D. R. Huffman, *Absorption and Scattering of Light by Small Particles* (Wiley, New York, 1983; Mir, Moscow, 1986).
46. J. M. Schmitt and G. Kumar, *Appl. Opt.* **37**, 2788 (1998).
47. V. S. Lee and L. Tarassenko, *J. Opt. Soc. Am. A* **8**, 1135 (1991).
48. M. A. Rozentul, *General Therapy of Skin Diseases* (Meditsina, Moscow, 1970) [in Russian].
49. *Human Physiology*, Ed. by R. F. Smidth and G. Thews (Springer, Berlin, 1989).
50. V. D. Malyshev, I. M. Andryukhin, V. S. Bakushin, *et al.*, *Anesteziol. Reanimatol.* **3**, 68 (1997).

*Translated by V. Rogovĭ*